

60 Years of the Loeb-Sourirajan Membrane
Principles, New Materials, Modelling, Characterization, and
Applications

Edited by: Hui-Hsin Tseng, Woei Jye Lau, ... Liang An

Elsevier

Radarweg 29, PO Box 211, 1000 AE Amsterdam, Netherlands
The Boulevard, Langford Lane, Kidlington, Oxford OX5 1GB, United Kingdom
50 Hampshire Street, 5th Floor, Cambridge, MA 02139, United States

Copyright © 2022 Elsevier Inc. All rights reserved.

No part of this publication may be reproduced or transmitted in any form or by any means, electronic or mechanical, including photocopying, recording, or any information storage and retrieval system, without permission in writing from the publisher. Details on how to seek permission, further information about the Publisher's permissions policies and our arrangements with organizations such as the Copyright Clearance Center and the Copyright Licensing Agency, can be found at our website: www.elsevier.com/permissions.

This book and the individual contributions contained in it are protected under copyright by the Publisher (other than as may be noted herein).

Notices

Knowledge and best practice in this field are constantly changing. As new research and experience broaden our understanding, changes in research methods, professional practices, or medical treatment may become necessary.

Practitioners and researchers must always rely on their own experience and knowledge in evaluating and using any information, methods, compounds, or experiments described herein. In using such information or methods they should be mindful of their own safety and the safety of others, including parties for whom they have a professional responsibility.

To the fullest extent of the law, neither the Publisher nor the authors, contributors, or editors, assume any liability for any injury and/or damage to persons or property as a matter of products liability, negligence or otherwise, or from any use or operation of any methods, products, instructions, or ideas contained in the material herein.

ISBN: 978-0-323-89977-2

For Information on all Elsevier publications
visit our website at <https://www.elsevier.com/books-and-journals>

Publisher: Susan Dennis
Acquisitions Editor: Anita Koch
Editorial Project Manager: Lindsay Lawrence
Production Project Manager: Sruthi Sathesh
Cover Designer: Victoria Pearson

Typeset by MPS Limited, Chennai, India



Preface

It has been over 60 years since the development of the first asymmetric polymeric membrane by Dr. Sidney Loeb and Dr. Srinivasa Sourirajan (University of California, Los Angeles, United States) for seawater desalination. Research in membrane science and technology has progressed rapidly over the past decades, and many new and advanced materials (both organic and inorganic) have been discovered and employed in the fabrication of membranes and the modification of their properties. It is therefore of paramount importance to summarize the fundamental understanding of and information about these membranes and their distinctive applications. In this book a comprehensive overview of membrane technology is presented, from the fundamental knowledge of fabrication principles and separation mechanisms to a wide range of applications, including new and emerging processes.

In more detail, this book provides essential guidance for students, researchers, and scientists working in the field of membrane science and technology. The fundamentals of membranes in different technologies, including their working principles, transport mechanisms, and requirements for practical applications, are discussed in this book. Key references and practical sources are also provided, enabling an in-depth understanding of the numerous aspects of membrane science and technology.

Furthermore, studies on membranes and their applications, such as in water and wastewater treatment, chemical and biomedical processes, gas separation, and renewable power generation, are reviewed in this book. For instance, recent advances in three-dimensional membranes for water applications, organosilica and metal-organic framework membranes for gas separation, high-performance membranes for vanadium redox flow batteries and vanadium-air redox flow batteries, ceramic membranes for fuel cells, and membranes with enhanced safety for lithium-ion batteries are summarized and discussed extensively. Recent advances in modeling and simulations of different membranes and their components, such as spiral-wound membranes and spacer-filled channels, are also included to provide better insights.

To facilitate a comprehensive characterization of membranes at different levels, the book also presents the common testing methods, along with some cutting-edge techniques for the accurate evaluation of the membrane properties and performances, which are of vital importance to the future development of advanced membranes. For instance, the advanced characterization for membrane surface fouling is discussed in detail.

Finally, to enable a better understanding of the latest trends and current research on membrane technology, the most up-to-date details on the use of advanced organic and inorganic materials and novel membrane fabrication techniques for the development of membranes are also reviewed. The advantages of these new materials along with the superiority of the newly developed fabrication methods in comparison to conventional strategies are also extensively discussed.

This book will equip future researchers with the ideas and directions that they need to understand the great potential and prospects of next-generation membrane fabrication. It is also the aim of this book to reflect the ample research activities and outcomes in the membrane field with an eye toward global utilization and impact.

This book is an essential reference resource not only for students and researchers but also for professionals and policymakers around the globe working in three main sectors: academia, industry, and government.

We would like to express our gratitude to all the authors who contributed to this book and shared their valuable state-of-the-art knowledge and experience with the associated topics. Last but not the least, we acknowledge the professional staff of Elsevier for their continuous support.

Hui-Hsin Tseng¹, Woei Jye Lau², Mohammad A. Al-Ghouthi³ and Liang An⁴

¹Department of Environmental Engineering, National Chung Hsing University, Taichung, Taiwan, ²Advanced Membrane Technology Research Centre (AMTEC), School of Chemical and Energy Engineering, Universiti Teknologi Malaysia, Skudai, Malaysia, ³Department of Biological and Environmental Sciences, College of Arts and Sciences, Qatar University, Doha, Qatar, ⁴Department of Mechanical Engineering, The Hong Kong Polytechnic University, Hong Kong, P.R. China

Contents

List of contributors	xvii
About the editors	xxv
Preface	xxvii
Chapter 1 Ionic liquid–based membranes for gas separation	1
<i>Eiji Kamio</i>	
1.1 Introduction.....	1
1.1.1 Ionic liquids	2
1.1.2 Gas permeability of room-temperature ionic liquid–based membranes	4
1.2 Ionic liquid–based CO ₂ separation membranes	8
1.2.1 Supported ionic liquid membranes	10
1.2.2 Pressure-resistant ionic liquid–based membranes.....	11
1.3 CO ₂ -reactive ionic liquid–based facilitated-transport membranes.....	17
1.3.1 Design concepts of CO ₂ -reactive ionic liquids and CO ₂ permeation mechanisms of CO ₂ -reactive ionic liquid–based supported ionic liquid membranes	17
1.3.2 Amine-functionalized ionic liquid–based supported ionic liquid membranes	18
1.3.3 Amino acid ionic liquid–based supported ionic liquid membranes	19
1.3.4 Supported ionic liquid membranes containing aprotic heterocyclic anion –based ionic liquids.....	21
1.3.5 Supported ionic liquid membranes containing ionic liquids with carboxylate anions.....	22
1.4 Ion gel membranes containing task-specific ionic liquids	23
1.4.1 Ion gel membranes containing amino acid ionic liquids and aprotic heterocyclic anion–based ionic liquids.....	23
1.4.2 Ion gel membranes with epoxy amine gel networks	25
1.5 Conclusion and remarks	26
References	26

Chapter 2	Zwitterionic polymers in biofouling and inorganic fouling mechanisms	33
	<i>Harout Arabaghian, Meng Wang, John Ordonez and Debora F. Rodrigues</i>	
2.1	Introduction.....	33
2.2	Zwitterionic membrane fabrication and characterization	37
2.2.1	Grafting processes for membrane modification	37
2.2.2	Membrane modification by in situ modification	42
2.3	Zwitterionic polymers and inorganic fouling	44
2.3.1	Zwitterionic polymers and ionic interactions.....	45
2.3.2	Mineral scaling on ZI-modified membranes	46
2.4	Zwitterionic polymers and organic fouling	47
2.4.1	The Mechanisms of zwitterionic polymers' resistance to organic fouling	48
2.4.2	The environmental conditions and organic foulants that influence zwitterionic polymers	51
2.5	Zwitterionic polymers and biofouling	53
2.5.1	Zwitterionic polymers and their interaction with prokaryotic cells.....	56
2.5.2	Zwitterionic polymers and their interaction with eukaryotic cells	60
2.6	Conclusions and further remarks	63
	Acknowledgement	65
	References	65
Chapter 3	Recent advances in 3D printed membranes for water applications.....	71
	<i>Wae Zin Tan, Chai Hoon Koo, Woei Jye Lau, Woon Chan Chong and Jing Yuen Tey</i>	
3.1	Introduction.....	71
3.2	3D printing technologies and classification	73
3.2.1	Directed energy deposition	74
3.2.2	Material jetting	74
3.2.3	Sheet lamination	76
3.2.4	Binder jetting.....	76
3.2.5	Material extrusion.....	76
3.2.6	Powder bed fusion	77
3.2.7	Vat Photopolymerization.....	77
3.2.8	Advantages and limitations of 3D printing methods.....	78
3.2.9	Role and trend of 3D printing in membrane technology for water applications.....	78
3.3	Applications of 3D printing in membrane technology.....	80
3.3.1	Membrane fabrication via direct 3D printing.....	81
3.3.2	Membrane surface modification via coating aided by 3D printing	83
3.4	Conclusion and future perspectives	94
	References	94

Chapter 4	A 15-year review of novel monomers for thin-film composite membrane fabrication for water applications	97
	<i>John Ogbe Origomisan, Ying Siew Khoo, Woei Jye Lau, Ahmad Fauzi Ismail and Adewale Adewuyi</i>	
4.1	Introduction.....	97
4.2	Commercial thin-film composite membranes	100
4.3	Novel amine monomers	101
4.3.1	Monomers bearing only $-NH_2$	101
4.3.2	Monomers Bearing $-NH_2/-OH$ and $-OH/-SO_3$	108
4.3.3	Monomers bearing multiple—hydroxyl groups	110
4.3.4	Monomers for improved chlorine stability.....	114
4.4	Novel acyl chloride monomers	115
4.4.1	Monomers with single/dual $COCl$	118
4.4.2	Monomers with three $COCl$ s	119
4.4.3	Monomers with Multiple $COCl$ s	122
4.5	Comparison of novel thin-film composite membranes with commercial membranes	123
4.6	Conclusion	125
	References	126
Chapter 5	Recent advances in high-performance membranes for vanadium redox flow battery.....	131
	<i>Jiaye Ye, Jun Su, Huiyun Li and Lidong Sun</i>	
5.1	Introduction.....	131
5.1.1	The development of redox flow batteries	131
5.1.2	The essential role of membrane in a vanadium redox flow battery	135
5.2	Inorganic modification	136
5.2.1	Zero-dimensional nanoparticles.....	136
5.2.2	One-dimensional nanowires/nanotubes.....	140
5.2.3	Two-dimensional nanosheets/nanoplates	143
5.3	Organic modification	145
5.3.1	Covalent modification	145
5.3.2	Noncovalent modification	146
5.4	Summary and outlook.....	148
	References	148
Chapter 6	Membranes for vanadium-air redox flow batteries.....	155
	<i>Xingyi Shi, Yanding Bi, Oladapo Christopher Esan and Liang An</i>	
6.1	Introduction.....	155
6.2	General description.....	158
6.2.1	Working principles	158
6.2.2	Functional requirements of membranes	158

6.3	Membrane classifications.....	159
6.3.1	Commercial Nafion membranes	159
6.3.2	Other membranes.....	160
6.4	Mechanisms and influences of species crossover.....	164
6.4.1	Oxygen permeation	164
6.4.2	Vanadium ion crossover	166
6.4.3	Water transport.....	168
6.5	Performance-enhancing strategies for membranes	169
6.6	Summary.....	171
	Acknowledgement	172
	References	172

Chapter 7 Carbon membrane for the application in gas separation:
recent development and prospects 177
Yu-Ting Lin, Ming-Yen Wey and Hui-Hsin Tseng

7.1	Introduction.....	177
7.2	Designs of carbon membrane.....	180
7.2.1	Geometrical classifications	180
7.2.2	Precursor selection for carbon membrane.....	182
7.2.3	Preparation of polymeric membrane.....	185
7.2.4	Pyrolysis procedure	188
7.2.5	Methods for tuning the pore dimension.....	190
7.2.6	Module construction	193
7.3	Gas transport mechanism.....	195
7.4	Microstructure characterization	198
7.4.1	Raman.....	198
7.4.2	X-ray photoelectron spectroscopy.....	198
7.4.3	X-ray diffraction	199
7.4.4	Focused ion beam and transmission electron microscopy.....	200
7.5	Overall performance review for each gas pair	200
7.5.1	Hydrogen purification	200
7.5.2	Carbon sequestration	203
7.5.3	Air separation	205
7.5.4	Natural gas sweetening.....	205
7.6	Conclusion and outlook	208
	Acknowledgment	208
	References	208

Chapter 8 Metal-organic framework membranes for gas separation
and pervaporation 215
*Dun-Yen Kang, Han-Lun Hung, Hsin-Yu Tsai, Jun-Yu Lai and
Ting-Hsiang Hung*

8.1	Introduction.....	215
8.2	Fabrication of pure metal-organic framework membranes	216
8.3	Metal-organic framework membranes for gas separations	220

8.4	Computational efforts on metal-organic framework membranes for gas separations.....	227
8.5	Metal-organic framework membranes for pervaporation.....	230
8.6	Conclusions and outlook	232
	References	233

Chapter 9 Advanced ceramic membrane design for gas separation and energy application 239

Tao Li, Mohamad Fairus Rabuni, Unalome Wetwatana Hartley and Kang Li

9.1	Introduction.....	239
9.1.1	Micro-structured ceramic membranes.....	240
9.1.2	Phase inversion–assisted fabrication.....	242
9.1.3	Micro-channel formation and micro-structure tailoring.....	243
9.2	Oxygen-permeable membrane and membrane reactor.....	245
9.2.1	Oxygen transport in high-temperature ion conductors	245
9.2.2	Design of high-performance oxygen permeation membrane	247
9.2.3	Catalytic reactor based on oxygen-permeable membrane	253
9.3	Ceramic membrane in energy applications.....	254
9.3.1	Solid oxide fuel cell.....	255
9.3.2	Coextrusion of functional membrane for high-performance micro-tubular-solid oxide fuel cells	257
9.3.3	New micro-monolithic solid oxide fuel cell and utilization of waste methane	258
9.4	Conclusion	263
	References	264

Chapter 10 Recent advances in lithium-ion battery separators with enhanced safety 269

Weiqiang Lv and Xingyi Zhang

10.1	Introduction	269
10.2	Self-shutdown separators.....	271
10.3	Mechanically strong separators	273
10.3.1	Increasing the tensile strength of separators.....	274
10.3.2	Increasing the puncture strength of separators.....	278
10.4	Nonflammable separators	280
10.4.1	Ceramic-coated fibrous separators	284
10.4.2	Separators with flame-retardant additives	286
10.5	All-solid-state electrolytes.....	289
10.5.1	Solid polymer electrolytes	289

10.5.2	Inorganic all-solid-state electrolytes.....	292
10.5.3	Composite organic–inorganic solid electrolytes.....	295
10.6	Future perspectives	297
	References	298

Chapter 11 Silicon-based subnanoporous membranes with amorphous structures

	<i>Toshinori Tsuru</i>	
11.1	Introduction	305
11.2	Development of subnanoporous membranes.....	306
11.2.1	Organosilica membranes.....	306
11.2.2	Silicon carbide–based membranes.....	309
11.2.3	Plasma-enhanced chemical vapor deposition membranes	309
11.3	Applications of membrane for gas phase separation.....	311
11.3.1	Application of silicon oxide–based membranes for gas separation.....	311
11.3.2	Application of silicon-based nonoxide membranes for gas separation.....	314
11.3.3	Application of membranes for high-temperature water vapor recovery.....	314
11.4	Applications of membranes for solvent separation	317
11.4.1	Evaluation of the separation energy of solvent mixture	317
11.4.2	Development and application of organic solvent nanofiltration membranes	319
11.4.3	Development and application of membranes for organic solvent reverse osmosis.....	321
11.5	Application to pervaporation	322
11.5.1	Pervaporation dehydration using organosilica membranes	323
11.5.2	Pervaporation of organic solvent mixtures	324
11.6	Conclusion	325
	References	325

Chapter 12 Ultrafiltration mixed matrix membranes: metal–organic frameworks as emerging enhancers

	<i>Mariam Ouda, Yazan Ibrahim, Hanaa Hegab, Fawzi Banat and Shadi W. Hasan</i>	
12.1	Introduction	329
12.2	Microenhancers and nanoenhancers	331
12.3	Antifouling and antibacterial properties	334
12.4	Dye rejection.....	339
12.5	Other applications.....	341
12.6	Conclusions and future outlook.....	344
	References	345

Chapter 13	Zwitterion-modified membranes for water reclamation	349
	<i>Gansheng Liu, Christine Matindi, Mengyang Hu, Xianhui Li, Xiaohua Ma and Jianxin Li</i>	
13.1	Introduction	349
13.2	Classification of zwitterionic polymers	351
13.2.1	Polybetaines	351
13.2.2	Polyampholytes	355
13.3	Antifouling mechanisms of zwitterionic units in membranes	357
13.3.1	Classification of membrane foulants	357
13.3.2	Establishment of a hydration layer on the membrane surface	358
13.3.3	Steric hindrance effect	359
13.4	Preparation of zwitterion-modified membranes	360
13.4.1	Modification by blending of zwitterionic polymers	360
13.4.2	Modification by grafting	363
13.4.3	Modification by surface coating	366
13.4.4	Modification by surface quaternization	367
13.5	Applications of zwitterion-modified polymer membranes	368
13.5.1	Treatment of natural organic matter in water	368
13.5.2	Oily wastewater treatment	370
13.5.3	Textile wastewater treatment	374
13.5.4	Desalination	375
13.6	Conclusion and prospects	377
	Acknowledgments	377
	References	377
Chapter 14	Modelling of spiral-wound membrane for gas separation: current developments and future direction	391
	<i>Abdul Aiman Abdul Latif, Kok Keong Lau and Serene Sow Mun Lock</i>	
14.1	Introduction	391
14.2	Construction and flow configuration of spiral-wound membrane	394
14.3	Modelling strategies	394
14.3.1	One-dimensional model	396
14.3.2	Two-dimensional model	399
14.3.3	Three-dimensional model	402
14.3.4	Summary of the mathematical models for spiral-wound membrane	405
14.4	Challenges and future direction in modelling of spiral-wound membrane in gas separation	408
14.4.1	Multicomponent separation	408

14.4.2	Effect of pressure drop in feed and permeate channel	408
14.4.3	Effect of heat transfer within the module	409
14.5	Conclusion	410
	References	410
Chapter 15	Modelling flow and mass transfer inside spacer-filled channels for reverse osmosis membrane modules	413
	<i>Yie Kai Chong, Yong Yeow Liang, Woei Jye Lau and Gustavo Adolfo Fimbres Weihs</i>	
15.1	Introduction	413
15.2	One-dimensional model	416
15.3	Two-dimensional model	418
15.4	Three-dimensional model	422
15.5	Conclusion	429
	Acknowledgment	430
	References	430
Chapter 16	Transport model-based prediction of polymeric membrane filtration for water treatment	433
	<i>Krishnasri V. Kurada and Sirshendu De</i>	
16.1	Introduction	433
16.2	Transport phenomena-based models	436
16.2.1	Osmotic pressure-based models	436
16.3	Gel layer—controlled mechanism	449
16.3.1	Transient one-dimensional gel layer controlling model coupled with film theory	449
16.3.2	Transient one-dimensional gel layer—controlling model coupled with a pore flow transport	452
16.3.3	Modelling of mixed matrix membranes	454
16.4	Conclusion	459
	References	460
Chapter 17	Molecular modelling and simulation of membrane formation	463
	<i>Zhen Wang, Sher Ling Lee, Tse-Chiang Huang, Geng-Sheng Lin, Tomohisa Yoshioka and Kuo-Lun Tung</i>	
17.1	Molecular modelling and simulation	463
17.1.1	Introduction	463
17.1.2	Types of simulation methods	464
17.1.3	Section conclusions	468
17.2	Modelling and simulations of membrane formation	468
17.2.1	Phase separation	469
17.2.2	Dry casting	476

17.2.3	Interfacial polymerization	476
17.3	Modelling and simulation on hollow-fiber membrane	479
17.3.1	Physical mass transfer model.....	479
17.3.2	Dissipative particle dynamics	481
17.3.3	Finite element method	482
17.4	Simulation and modelling in membrane design	482
17.4.1	Graphene and two-dimensional carbon material	482
17.4.2	Zeolite imidazolate framework and metal-organic membranes	485
17.5	Future trends in molecular simulations of membrane formation	489
	References	491

Chapter 18 Advanced characterization of membrane surface fouling 499
Kang Xiao, Yirong Xu, Xuyang Cao, Hao Xu and Yufang Li

18.1	Introduction	499
18.2	Modelling of surface fouling	500
18.2.1	Filtration laws	500
18.2.2	Compression of surface foulant layer.....	502
18.2.3	Maturation and retardation of surface foulant layer	503
18.2.4	Concentration polarization boundary layer	503
18.3	Online characterization of surface fouling	504
18.3.1	Direct observation.....	504
18.3.2	Optical coherence tomography.....	505
18.3.3	Attenuated total reflection–Fourier transform infrared spectroscopy.....	506
18.3.4	Raman spectroscopy	506
18.3.5	Fluorescence spectroscopy	507
18.3.6	Electrochemical impedance spectroscopy	509
18.3.7	Quartz crystal microbalance with dissipation	510
18.3.8	Surface plasmon resonance	510
18.3.9	Light sheet fluorescence microscopy	511
18.4	Offline characterization of surface fouling	511
18.4.1	Microscopic methods	511
18.4.2	Spectroscopic methods	513
18.4.3	Other methods	519
18.4.4	Further data mining via statistical analysis	521
18.5	Characterization of extracts from the surface foulant layer 521	
18.5.1	Extraction of surface foulants	522
18.5.2	Chemical composition	522
18.5.3	Physicochemical properties.....	522
18.5.4	Spectroscopic properties	523
18.5.5	Chromatography	524
18.5.6	Biological properties	525
18.6	Concluding remarks	526
	References	527

Chapter 19	Reverse osmosis membrane fouling and its physical, chemical, and biological characterization	533
	<i>Mohammad Yousaf Ashfaq and Mohammad A. Al-Ghouti</i>	
19.1	Introduction	533
19.2	Types of membrane fouling	534
19.2.1	Biofouling	535
19.2.2	Inorganic fouling/scaling.....	538
19.2.3	Organic fouling.....	541
19.2.4	Colloidal/particulate fouling	541
19.3	Membrane fouling characterization	542
19.3.1	Microscopic techniques.....	544
19.3.2	Spectroscopic and analytical techniques.....	553
19.4	Conclusions	565
	Acknowledgment	566
	References	566
Chapter 20	Current status of ion exchange membranes for electro dialysis/reverse electro dialysis and membrane capacitive deionization/capacitive mixing	575
	<i>Nalan Kabay, Enver Güler, Katarzyna Smolinska-Kempisty and Marek Bryjak</i>	
20.1	Ion exchange membranes in electro dialysis and membrane capacitive deionization systems for water demineralization	575
20.1.1	Introduction	575
20.1.2	Electro dialysis.....	576
20.1.3	Membrane capacitive deionization	583
20.2	Ion exchange membranes for harvesting salinity gradient energy	586
20.2.1	Introduction	586
20.2.2	Reverse electro dialysis	587
20.2.3	Capacitive mixing	592
20.3	Conclusion and future perspectives.....	594
	Acknowledgments.....	594
	References	595
Chapter 21	Reverse osmosis membrane scaling during brackish groundwater desalination.....	603
	<i>Kai-Ge Lu, Haiou Huang and Mengya Li</i>	
21.1	Introduction	603
21.2	Established theories for membrane-scaling formation	604
21.2.1	Scaling thermodynamics.....	604
21.2.2	Scaling kinetics.....	605
21.3	Membrane scaling in brackish groundwater desalination....	607
21.3.1	Brackish groundwater quality	607

21.3.2	Scaling types and morphology.....	608
21.3.3	Effects of water quality on mineral scaling.....	610
21.3.4	Relationships between membrane scaling and permeate flux.....	612
21.4	Control strategies for membrane scaling	613
21.4.1	Feedwater pretreatment.....	613
21.4.2	Antiscalants.....	613
21.4.3	Operation mode of reverse osmosis system.....	615
21.4.4	Scaling-resistant reverse osmosis membrane.....	616
21.5	Future challenges for mineral-scaling control.....	618
	References	620

Chapter 22 Ceramic membrane in a solid oxide fuel cell–based gas sensor 627
Sutida Marthosa and Montri Luengchavanon

22.1	Introduction	627
22.2	Research progress on ceramic membrane.....	631
22.3	Issues in developing a micro-solid oxide fuel cell methane sensor	634
22.4	High temperature O-ring in a fuel cell testing station.....	636
22.4.1	Current situation.....	636
22.4.2	O-ring characteristics	636
22.4.3	O-ring performance and thermally resistive filler.....	638
22.5	Micro-solid oxide fuel cell methane sensor	639
22.5.1	Current situation.....	639
22.5.2	Sensor development overview.....	640
22.5.3	Design and character of the sensor.....	640
22.5.4	Sensor development.....	642
22.6	Conclusion	646
	Acknowledgment	647
	References	647

INDEX 651

Modelling flow and mass transfer inside spacer-filled channels for reverse osmosis membrane modules

Yie Kai Chong¹, Yong Yeow Liang¹, Woei Jye Lau² and
Gustavo Adolfo Fimbres Weihs³

¹College of Engineering, Universiti Malaysia Pahang, Lebuhraya Tun Razak, Gambang, Kuantan, Pahang, Malaysia, ²Advanced Membrane Technology Research Centre (AMTEC), School of Chemical and Energy Engineering, Universiti Teknologi Malaysia, Skudai, Malaysia, ³The University of Sydney, School of Chemical and Biomolecular Engineering, NSW, Australia

CONTENTS

15.1	Introduction	... 413
15.2	One-dimensional model 416
15.3	Two-dimensional model 418
15.4	Three-dimensional model 422
15.5	Conclusion 429
	Acknowledgment 430
	References 430

15.1 Introduction

Desalination has progressed rapidly since the 1980s as freshwater is becoming more scarce as a result of the fast-growing population size and global climate change. To relieve this situation, membrane processes are recognized as promising approaches to purifying brackish and ocean water to meet the global water demand. Among the membrane technologies, reverse osmosis (RO) has gained the most attention and is used in half of the desalination plants in the world (Goh et al., 2018; Qasim et al., 2019). RO is used in water purification to effectively remove unwanted solutes (particularly dissolved ions) in the water by means of membrane permeation. The global RO membrane market was \$6.9 billion in 2017 and is estimated to show an almost double increase by 2025 (Toh et al., 2020a).

Spiral-wound membrane (SWM) modules were invented in the 1960s and have become one of the most common membrane arrangements for water applications. SWMs are composed of membrane leaves, feed spacers, permeate spacers, and a permeate tube. For their construction, the membrane leaves are first folded in half to form an envelope. The permeate spacer is then inserted into the envelope to form the permeate channel, with the sides glued together to force the permeate to flow in the direction of the permeate tube. Next, a feed spacer is inserted between a pair of membrane envelopes to form a feed channel. These steps are repeated to form several membrane layers, and these layers are wrapped spirally to form a cylindrical module, as

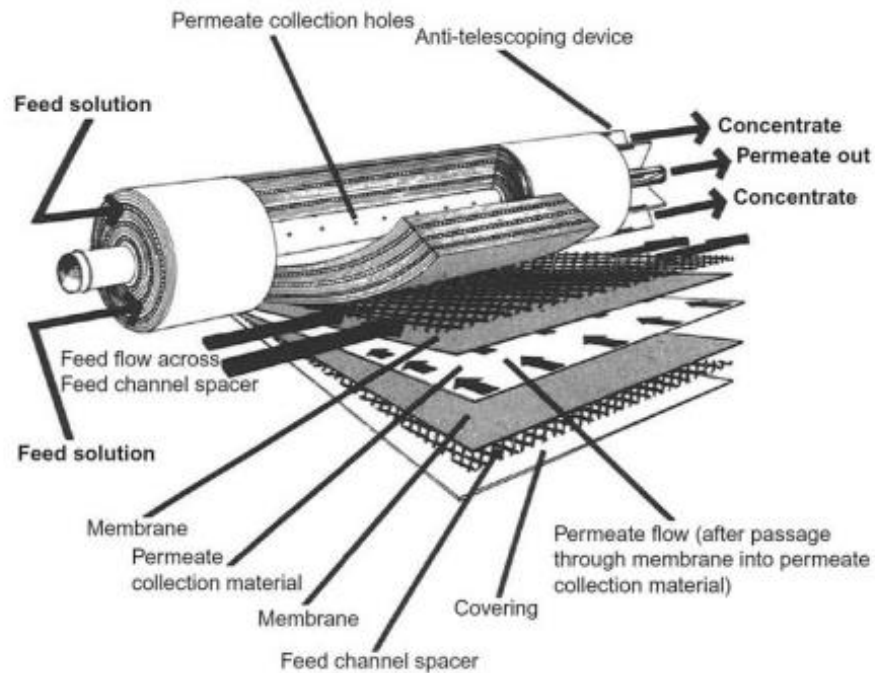


FIGURE 15.1
Configuration of spiral-wound membrane for reverse osmosis (Sparks & Chase, 2016).

depicted in Fig. 15.1 (Sparks & Chase, 2016). The feed passes through the feed channel, and the water selectively permeates across the RO membrane to the permeate channel as the result of applied pressure, overcoming the osmotic pressure. The rejected salt becomes concentrated in the feed channel solution, forming the brine that exits the module from the opposite side of the feed channel. The purified water exits the module via the permeate tube as permeate.

The SWM design offers several benefits, such as (1) high packing density to give larger surface area per volume (Qasim et al., 2019), (2) low manufacturing and operating costs compared to flat plate and tubular modules (Belfort, 1988; El-Ghaffar & Tiema, 2017), and (3) being more robust against membrane breakage compared to hollow-fiber membrane (Lu & Chung, 2019). However, concentration polarization and fouling are common serious problems in SWMs.

To reduce the drawbacks associated with RO membrane operations and to optimize SWM performance in water desalination, intensive experimental studies have been conducted through approaches such as varying the feed

conditions (Goosen et al., 2002; Madaeni & Koocheki, 2006) or modifying the geometrical structure of SWMs (Sablani et al., 2002). Although less intrusive experimental methods (e.g., particle image velocimetry) have been developed, the resolution of those methods is insufficient to study the mass transport within the boundary layer (Fimbres-Weihs & Wiley, 2010). Therefore CFD aids the process by nonintrusively visualizing the intricate local and time dependent phenomena of flow and mass transfer enhancement.

Initially the modelling of SWMs for RO membrane operations was focused on prediction of the permeate flux and permeate concentration. One-dimensional (1D) models have been developed through either numerical or analytical solutions based on the fundamental concepts of mass and momentum balance. Since the 2000s, computers have faster rates of calculation and can access larger memory sizes, making it possible to solve larger and more complex problems. Since then, CFD has become a powerful and reliable tool to simulate fluid flow and to provide high-resolution visualization of hydrodynamic and concentration profiles inside the feed channel of SWMs. The SWM feed channel was first modeled as two-dimensional (2D) in the early 2000s, then evolved into three-dimensional (3D) models with greater resolution. Fig. 15.2 summarizes the evolution of CFD studies for RO feed spacers. In view of the significant progress of modelling flow and mass transfer inside spacer-filled channels for RO membrane modules, the chapter aims to discuss the recent research of these one-dimensional (1D), 2D, and 3D simulation models, followed by the studies of unsteady shear strategies, novel spacer geometries, and fouling reduction.

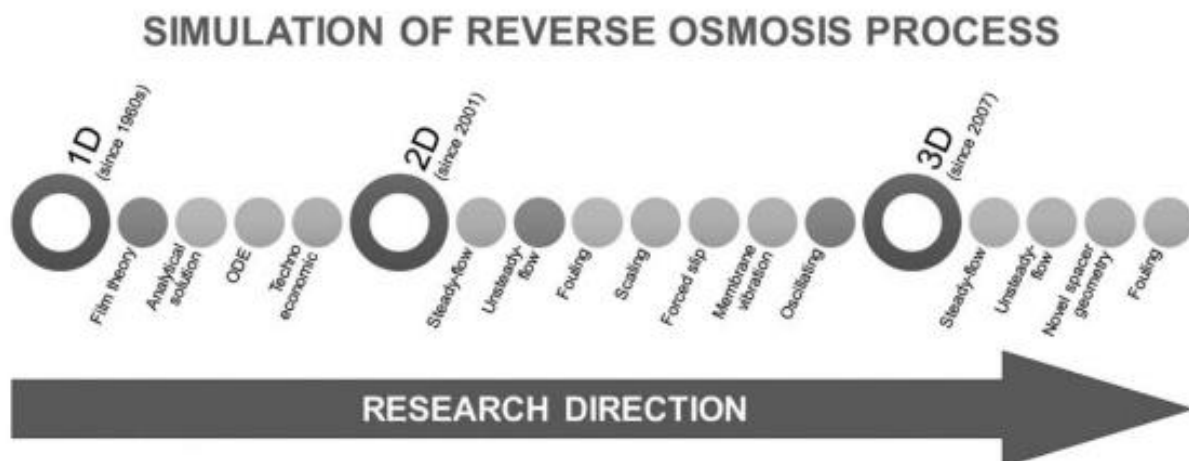


FIGURE 15.2

The research direction of the simulation of reverse osmosis process since the 1900s.

15.2 One-dimensional model

In RO systems, solvent transport is driven by the pressure gradient and resisted by the osmotic pressure. At the same time, the dissolved solutes move toward the membrane through convective flux and move away from the membrane through diffusive flux due to membrane rejection. This leads to the accumulation of rejected solute near the membrane surface, forming a concentration boundary layer, which is also known as CP. Film theory assumes mass balance at a steady state, such that the convective flux of solute is equal to the diffusive flux of solute:

$$J(C - C_p) - D_s \frac{dC}{dy} = 0 \quad (15.1)$$

where J is the permeate flux, C is the solute concentration, and D_s is the solute diffusivity. By integrating Eq. (15.1) with the boundary conditions $C = C_w$ at $y = 0$ and $C = C_b$ at $y = \delta$, the CP modulus can be expressed as:

$$\gamma = \frac{C_w - C_p}{C_b - C_p} = \exp\left(\frac{J}{k_{mt}}\right) \quad (15.2)$$

where the mass transfer coefficient, $k_{mt} = D_s/\delta$.

Film theory gives a simplified view of the concentration profile in a boundary layer of thickness δ , which is located between the membrane wall and the bulk solution, as shown in Fig. 15.3. This theory assumes that the axial solute convection near the membrane wall and the local changes of liquid density can be neglected.

However, the simplicity of film theory has some limitations, as it neglects several effects, including the axial convection term near the membrane wall,

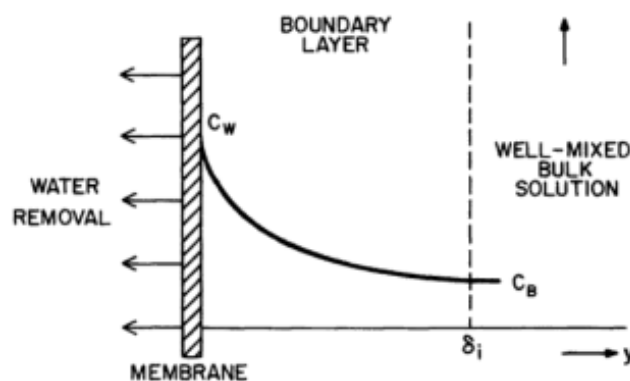


FIGURE 15.3
Concentration profile in boundary layer (Blatt et al., 1970).

Index

Note: Page numbers followed by “f” and “t” refer to figures and tables, respectively.

A

- Ab initio methods, 464–466
- Absorption, 1
- Accelerated precipitation softening (APS), 615
- Acid gas removal process, 391
- Acid impurities, 205
- Acyl chloride monomers, 115–123
 - monomers with multiple COCl₂, 122–123
 - monomers with single/dual COCl₂, 118–119
 - monomers with three COCl₂, 119–122
 - used for thin-film composite membrane fabrication, 116t
- Additive manufacturing, 73–74
- Adenosine triphosphate (ATP), 525
- Adsorption, 1, 613
- Adsorptive resistance, 456
- Air separation, 205, 245
- Aliphatic diamine PIP, 100–101
- Alkaline fuel cells (AFCs), 627
- All-solid-state electrolytes (ASSEs), 289–297
 - composite organic–inorganic solid electrolytes, 295–297
 - inorganic all-solid-state electrolytes, 292–294
 - solid polymer electrolytes, 289–291
- Allylhydridopolycarbosilane (AHPCS), 309
- Alphaproteobacteria, 538
- Aluminum oxide (Al₂O₃), 279
- Aluminum-air batteries, 156
- American Society for Testing and Materials (ASTM), 74
- Amine monomers, 100–115
 - monomers bearing multiple—hydroxyl groups, 110–114
 - monomers bearing only—NH₂, 101–108
 - monomers bearing—NH₂/—OH and—OH/—SO₃, 108–110
 - monomers for improved chlorine stability, 114–115
 - for thin-film composite membrane fabrication, 102t
- Amine-functionalized IL–based supported IL membranes, 18–19
- Amino acid ILs (AAILs), 19. *See also* Room-temperature ILs (RTILs)
 - amino acid ionic liquid–based supported ionic liquid membranes, 19–21
 - ion gel membranes containing amino acid ionic liquids, 23–25
- Amino acids, 541
- Amino-functionalized Nafion(NH₂-Nafion), 143–145
- 4-aminophenyl sulfone (APS), 106–107
- 3-aminopropyltriethoxysilane, 222
- Ammonia, 201–203
- Ammonium polyphosphate (APP), 288
- Amorphous structure, 305–306
- Anion exchange membrane (AEMs), 578
- Anode composite, 641–642
- Anode functional layer (AFL), 257
- Anodic aluminum oxide (AAO), 219
- Antifouling mechanisms of zwitterionic units in membranes, 357–359
- Antiscalants, 613–615
- Aprotic heterocyclic anions (AHAs), 21–22
 - aprotic heterocyclic anion–based ionic liquids, 21–22
 - ion gel membranes containing AHA–based ionic liquids, 23–25
- Argon (Ar), 309–311
- Aromatic MPD, 100–101
- Aromatic TFC membrane, 97–98
- Asymmetric CA membrane, 97–98
- Asymmetrical-flow field-flow fractionation (AF₄), 524
- Atmospheric pressure PECVD (AP-PECVD), 309–311
- Atom transfer radical polymerization (ATRP), 37–39, 352
- Atomic force microscopy (AFM), 512, 549–550, 551f, 606
- Atomistic-scale methods, 466–467
 - MD simulation, 466
 - Monte Carlo simulation, 467
- Attenuated total reflection technology (ATR technology), 506
- Avizo (software), 262–263
- Axial direction, 400

B

- Bacillus licheniformis*, 58–59
- Bacillus* sp., 554
- Back diffusion process, 537–538
- Bacteroidetes*, 535

- Barium calcium aluminum borosilicate glass (BCABS), 635
- 4,4',4''-[benzene-1,3,5-triyltris(oxy)]tribenzoyl chloride (BTTC), 121–122
- 1,4-benzenedimethanol, 162–163
- 2,2'-benzidinedisulfonic acid (BDSA), 108–110
- Beta-cyclodextrin (β -CD), 111–113
- Betaproteobacteria*, 538
- Binary separation system, 396–397
- Binder jetting process (BJ process), 74, 76
- Biofilm, 54–55
- formation
- factors affecting, 537–538
- steps in, 535–537
- Biofouling, 335, 535–538
- zwitterionic polymers and, 53–63
- interaction with eukaryotic cells, 60–63
- interaction with prokaryotic cells, 56–59
- Biogas, 628–629, 639, 645–646
- Biological properties, 525
- Bioluminescence, 561
- Biotechnology, 577–578
- 2,2',4,4', 6,6'-biphenyl hexaacyl chloride (BHAC), 122–123
- 2,3',4,5',6-biphenyl pentaacyl chloride (BPAC), 122–123
- 2,4,4',6-biphenyl tetraacyl chloride (BTAC), 122–123
- Bipolar membranes for electrodialysis, 580–582
- 2,2'-bis(1-hydroxyl-1-trifluoromethyl-2,2,2-trifluoroethyl)-4,4'-methylenedianiline (BHTTM), 115
- 4,6-bis(3-[triethoxysilyl]-1-propoxy)-1,3-pyrimidine, 313–314
- Bis(triethoxysilyl) acetylene (BTESA), 321–322
- Bis(triethoxysilyl) ethane (BTESE), 308
- Bis(triethoxysilyl) methane (BTESM), 308
- Born-Oppenheimer approximation, 466
- Bovine serum albumin (BSA), 48, 110, 335, 362, 506, 619–620
- Brackish groundwater desalination, 607–612
- brackish groundwater quality, 607–608
- relationships between membrane scaling and permeate flux, 612
- scaling types and morphology, 607*t*, 608–610
- water quality effects on mineral scaling, 610–612
- Brackish surface water, 603
- Brackish water, 603
- Brackish water reverse osmosis (BWRO), 417
- bromo-2-methyl-N-(3-[triethoxysilyl]propyl) Ψ 2- Ψ , 362–363
- BSA. Bovine serum albumin; *See* Bovine serum albumin (BSA)
- Bulk crystallization, 608
- ## C
- Cahn-Hilliard model (CH model), 469–470
- Calcite, 608
- Calcium carbonate (CaCO_3), 357–358
- Calcium ions (Ca^{2+}), 539
- Calcium sulfate (CaSO_4), 357–358
- Calibration of methane concentration, 644–645
- Candida albicans*, 60–61
- Capacitive deionization (CDI), 344, 583, 603
- Capacitive Donnan Potential (CDP), 592
- Capacitive Double Layer Expansion (CDLE), 592
- Capacitive mixing, 592–593
- Carbohydrates, 541
- Carbon black (CB), 636
- Carbon dioxide (CO_2), 313–314, 391, 408
- CO_2 -reactive ionic liquid-based facilitated transport membranes, 17–23
- AAIL-based supported ionic liquid membranes, 19–21
- amine-functionalized ionic liquid-based supported ionic liquid membranes, 18–19
- CO_2 permeation mechanisms of CO_2 -reactive IL-based supported IL membranes and, 17–18
- SILMs containing aprotic heterocyclic anion-based ionic liquids, 21–22
- SILMs containing ionic liquids with carboxylate anions, 22–23
- diffusivity, 8
- emission, 1, 177–178, 203–205
- ionic liquid-based CO_2 separation membranes, 8–17
- pressure-resistant ionic liquid-based membranes, 11–17
- SILMs, 10–11
- separation membranes, 2
- Carbon membrane, 178–179
- designs, 180–195
- carbon membrane types in configuration and optical images, 181*f*
- comparison of different configuration, 182*t*
- geometrical classifications, 180–182
- methods for tuning pore dimension, 190–193
- module construction, 193–195
- precursor selection for carbon membrane, 182–185
- preparation of polymeric membrane, 185–188
- pyrolysis procedure, 188–190
- evolution process for, 179*f*
- gas transport mechanism, 195–197
- micro-structure characterization, 179–180, 198–200
- FIB and TEM, 200
- Raman spectroscopy, 198
- XPS, 198
- XRD, 199–200
- overall performance review for
- each gas pair, 200–207
- air separation, 205
- carbon sequestration, 203–205
- hydrogen purification, 200–203
- natural gas sweetening, 205–207
- separation performance of, 202*t*, 204*t*, 206*t*, 207*t*

- Carbon molecular sieving membrane, 195–197
 - Carbon nanotubes, 331
 - Carbon sequestration, 203–205
 - Carbon-based nanoparticles, 331
 - Carbonates (CO₃), 538–539, 632–633
 - Carbonization, 178–179, 185, 188–190
 - variables of carbonization condition and corresponding consequences, 189*t*
 - Carboxybetaine (CB), 33–34, 351–352
 - Carboxylate, 33–34
 - Carboxylic acids (COOH), 535, 578
 - Carboxymethyl cellulose (CMC), 615
 - Carrier transport membranes, 17
 - Cathodic catalyst, 631
 - Cation exchange membranes (CEMs), 578
 - Cellphones, 269
 - Cellulose acetate (CA), 88, 97–98, 469–470
 - Cellulose fibers (CFs), 284–286
 - Cellulose-based RO, 97
 - Ceramic electrolyte, 631
 - Ceramic fuel cells. *See* Solid oxide fuel cells (SOFCs)
 - Ceramic membrane, 72
 - design
 - ceramic membrane in energy applications, 254–263
 - micro-channel formation and micro-structure tailoring, 243–244
 - micro-structured ceramic membranes, 240–242
 - oxygen-permeable membrane and membrane reactor, 245–254
 - phase inversion–assisted fabrication, 242–243
 - in energy applications, 254–263
 - coextrusion of functional membrane, 257–258
 - new micro-monolithic solid oxide fuel cell and utilization of waste methane, 258–263
 - solid oxide fuel cell, 255–256
 - high temperature O-ring in fuel cell testing station, 636–639
 - current situation, 636
 - O-ring characteristics, 636–638
 - O-ring performance and thermally resistive filler, 638–639
 - issues in developing micro-solid oxide fuel cell methane sensor, 634–636
 - micro-solid oxide fuel cell methane sensor, 639–646
 - research progress on, 631–634
 - three-dimensional characterization of, 260–263
 - Ceramic micro-tubes, 244
 - Ceramic-coated fibrous separators, 284–286
 - Ceramic-coated separators, 271
 - Ceria oxide (CeO₂), 632
 - Ceria-carbonate ceramic electrolyte, 632–633
 - Characterization techniques, 534
 - Chemical synthesis, 245
 - Chemical vapor deposition (CVD), 191
 - Chlorella vulgaris*, 60–61
 - Chloride (Cl), 547–549
 - Chromatography, 524, 565
 - AF₄, 524
 - and mass spectrometry, 524
 - reversed-phase chromatography, 524
 - size-exclusion chromatography, 524
 - Coagulation, 613
 - Coarse-grained methods, 467–468
 - Coating techniques, 187–188
 - Cobalt (Co), 305–306, 634
 - Coextrusion of functional membrane, 257–258
 - Colloidal silica, 609–610, 612
 - Colloidal/particulate fouling, 541–542
 - Combined heat and power process, 255
 - Commercial membranes, 584–585
 - modules, 392
 - Commercial Nafion membranes, 159–160
 - Commercial thin-film composite membranes, 100–101
 - Competitive adsorption, 616–617
 - Composite organic–inorganic solid electrolytes, 295–297
 - Computational fluid dynamics methods (CFD methods), 402, 414–415
 - Concentration boundary layer, 416
 - Concentration polarization (CP), 416, 433, 503
 - boundary layer, 503–504
 - Conditioning film development, 535–536
 - Confocal laser scanning microscopy (CLSM), 513, 544–546, 545*f*
 - Congo red (Cr), 374
 - Contact angle (CA), 519–520
 - Conventional CO₂ separation methods, 1
 - Conventional fabrication methods, 72–74
 - Copolymers, 351
 - COSMO-RS method, 6
 - Coulombic efficiency, 165–167
 - Covalent modification, 145–146
 - Covid-19 pandemic, 575
 - CP. Concentration polarization; *See* Concentration polarization (CP)
 - Crossflow filtration, 501–502
 - Crossflow velocity, 537–538
 - Crosslinked GO (CLGO), 143–145
 - Crosslinking process, 162–163
 - Crossover phenomenon, 164
 - Cryogenic distillation technology, 245
 - Custom-made membranes, 585–586
 - composite electrodes with ion exchange property, 586
 - homogeneous membranes, 585
 - ion exchange membrane layers with nanoparticles, 586
 - pore-filling membranes, 586
 - 1,3-cyclohexanebis(methylamine) (CHMA), 114–115
- D**
- D-band, 198
 - Darcy's law, 434–435, 612
 - Data mining via statistical analysis, 521
 - Defect-free carbon membrane, 178–179
 - Defect-free polymeric membrane, 185
 - Deionized water (DI), 358–359

- Demineralization, 575–586
 for harvesting salinity gradient energy, 586–593
 membrane capacitive deionization, 583–586
- Density functional theory (DFT), 464–465
- Department of Defense (DOD), 628
- Desalination technologies, 71, 375–376, 376*f*, 413
- Detachment and dispersion, 537
- Diamines, 99
- 3,5-diamino-N-(4-aminophenyl) benzamide (DABA), 101–105, 104*f*
- 4,4-diaminodiphenylmethane (DADPM), 108, 109*f*
- Diethyl ally phosphate (DEAP), 287–288
- Differential interference contrast microscopy (DICM), 552
- Differential scanning calorimeter (DSC), 280–281
- Diffusive flux, 416
- Dimensionless constants, 397
- Dimethyl carbonate (DMC), 321–322, 324
- Diphenyl sulfone (DPS), 279
- Direct ink writing method (DIW method), 72
- Direct methanol fuel cells (DMFCs), 627–628
- Direct observation (DO), 504–505
- Directed energy deposition (DED), 74
- Dissipative particle dynamics (DPD), 467, 481
- Dittus-Boelter equation, 437
- Dodecyl trimethylammonium chloride (DTMA), 53
- Donnan exclusion principle, 447
- Donnan potential, 447
- Doping method, 245–247
- Double-distilled water (DDW), 370
- Dry casting method, 476
- Dry methane reforming reaction (DMR reaction), 645–646
- Dye rejection process, 339–341, 342*t*
- Dynamic viscosity, 418–419
- E**
- Electric field (EF), 165
- Electrically rechargeable liquid fuel system (e-fuel system), 170–171
- Electrochemical impedance spectroscopy (EIS), 509–510
- Electrodeionization (EDI), 575.
See also Membrane capacitive deionization (MCDI)
- Electrodialysis (ED), 575–586
 applications, 577–578
 membranes, 578–583
 bipolar membranes for electrodialysis, 580–582
 electrodialysis membranes with nanoparticles, 582–583
 monovalent-selective electrodialysis membranes, 580
 profiled electrodialysis membranes, 579–580
 setup, 577*f*
- Electromembrane processes, 575
- Electron microscopy, 543
- Electronic scale methods, 464–466
- Electroosmotic convection (EOC), 165
- Electroosmotic drag, 168
- Electroosmotic flow (EOF), 421–422
- Electrophoretic deposition (EPD), 274–275
- Electrospinning method, 280–281
- Electrostatic repulsion, 616–617
- Energy balance, 400
- Energy dispersive spectroscopy (EDS), 546–547
- Energy dispersive X-ray technique (EDX technique), 546–547
- Energy recovery device (ERD), 417
- Energy spectroscopy, 557
- Energy storage, 131
 capacity, 155–156
 system, 170–171
- Energy-dispersive X-ray spectroscopy (EDS), 513
- Energy-efficient membrane technology, 71
- Environmental conditions and organic foulants, 51–53
- Environmental scanning electron microscopy (ESEM), 511–512, 552
- Epilicoccus nigrum*, 60–61
- Epifluorescence microscopy, 550–552
- Epoxy amine gel networks, ion gel membranes with, 25
- Escherichia coli*, 86–88, 366
- Ethane (CH₃), 408
- 1-ethyl-3-methylimidazolium tetracyanoborate, 6
- 1-ethyl-3-methylimidazolium triluoromethanesulfonate (EMITFSI), 295
- Ethylene propylene diene monomer (EPDM), 636
- Eukaryotic cells, ZI polymers and interaction with, 60–63
- Ex situ scale observation detector (EXSOD), 606
- Excitation–emission matrix (EEM), 507–509
- Extended Nernst-Planck equation, 446
- Extended X-ray absorption fine structure (EXAFS), 519
- Extracellular polymeric substances (EPS), 535
- Extrusion process, 242
- F**
- Fabrication process, 587
- Facilitated-transport membrane, 17
- 6FDA/BPDA-DAM, 182–185
- Feed-flow reversal (FFR), 615–616
- Fick's law, 403
- Fick–Henry model, 401
- Film theory, transient one-dimensional gel layer controlling model with, 449–452
- Filtration laws, 500–502
- Finite difference method (FD method), 467
- Finite element method, 482
- Flat configuration, 181–182
- Flory-Huggins model, 469–470
- Flow through rectangular channel, 439–443
- Fluid density, 417–419
- Fluorescein isothiocyanate-conjugated bovine serum albumin (BSA-FITC), 108
- Fluorescence spectroscopy, 507–509
- Fluorine (F), 90–94, 305–306
- Fluorometry techniques, 560–561
- Flux recovery rate (FRR), 106, 360–361
- Foam materials, 269
- Focused ion beam (FIB), 198, 200
- Foregoing tuning methods, 191–193

- Forward osmosis (FO), 37–39, 100, 368–369, 603
- Fouling mechanisms, 424, 582
- Fourier transform infrared photoacoustic spectroscopy (FTIR/PAS), 562
- Fourier transform infrared spectroscopy (FTIR), 182–185, 506, 553–554, 554*f*
- Friction coefficient, 398
- Friction factor, 417
- Front-face excitation–emission matrix (FF-EEM), 514–515
- Fuel cell, 627
- ## G
- G-band, 198
- Gadolinium doped ceria (GDC), 630, 632
- Gadolinium oxide (Gd₂O₃), 632
- Gammaproteobacteria*, 538
- Gas chromatography (GC), 645
- Gas chromatography–mass spectrometry (GC–MS), 524
- Gas permeability of RTIL–based membranes, 4–8
- CO₂ diffusivity, 8
- CO₂ solubility, 5–6
- solubility selectivity of CO₂ in RTIL and permselectivity of CO₂, 6–7
- Gas phase separation, membrane applications for, 311–316
- membranes for high-temperature water vapor recovery, 314–316
- silicon oxide–based membranes for, 311–314
- silicon-based nonoxide membranes for, 314
- Gas separation
- metal-organic framework membranes for, 220–227
- computational efforts on, 227–230
- separation performance for CO₂/CH₄, 225*f*
- separation performance for CO₂/N₂, 224*f*
- separation performance for H₂/CO₂, 223*f*
- separation performance for H₂/N₂, 220*f*, 221*f*
- spiral-wound membrane in, 408–409
- Gas transport mechanism, 195–197, 196*f*
- Gaussian stochastic field, 470–471
- Gel layer–controlled mechanism, 449–459
- gel polarization of two-component system, 449*f*
- modeling of MMM, 454–459
- transient one-dimensional gel layer controlling model coupled with film theory, 449–452
- coupled with pore flow transport, 452–454
- Gel polymer separators, 270
- Gel-vapor deposition, 219
- Generalized 2DCOS, 521
- Geothermal energy, 177–178
- Gibbs-Duhem equation, 475
- Global warming, 203–205
- Glutaraldehyde, 589–590
- Grafting processes for membrane modification, 37–42
- Grafting-from process, 37–40
- Grafting-onto process, 37, 40–42
- Gram-negative bacteria, 535
- Graphene, 331, 482–485
- Graphene oxide (GO), 143, 331, 362
- Graphene with cysteine (CGO), 369–370
- Graphitic carbon nitride (g-C₃N₄), 143
- Gravimetric analysis, 562–564
- Greenhouse gas, 177–178
- abatement, 260
- and clean energy generation using ceramic fuel cells, 261*f*
- Greenhouse phenomenon, 203–205
- Gypsum (CaSO₄ 2H₂O), 609
- ## H
- Heat recovery system, 255
- Henry's law constant (MPa), 5
- of typical ionic liquids, 5*t*
- Hexamethyldisiloxane (HMDSO), 309–311
- High-performance liquid chromatography (HPLC), 565
- high-performance micro-tubular-solid oxide fuel cells, 257–258
- High-performance oxygen permeation membrane, design of, 247–252
- micro-tubes with open-channel micro-structure design, 247–248
- multichannel design for highly robust oxygen permeation membrane, 248–251
- new bio-inspired design for next-generation oxygen separation, 251–252
- High-temperature ion conductors, oxygen transport in, 245–247
- High-temperature water vapor recovery, membranes for, 314–316
- Higher-molecular-weight solutes (HMW solutes), 435
- “Hole-pillar spacer”, 425
- Hollow fiber configuration, 181–182
- Hollow-fiber membrane (HFM), 392, 479
- modeling and simulation on, 479–482
- dissipative particle dynamics, 481
- finite element method, 482
- physical mass transfer model, 479–480
- Homogeneous membranes, 585
- Humic acid (HA), 335, 619–620
- Hyaluronic acid (HA), 366
- Hybrid 2DCOS, 521
- Hybrid flow battery, 134–135
- Hydration layer on membrane surface, 358–359
- Hydrocracking, 200–201
- Hydroelectric power, 177–178
- Hydrogen (H₂), 239, 255, 629–630
- energy, 177–178
- purification, 200–203
- Hydrogen sulfide (H₂S), 391, 408
- Hydrophilic modification of membranes, 349–350
- Hydrotreating, 200–201
- 4-hydroxy-2,2,6,6-tetramethylpiperidin-1-oxyl (4-HO-TEMPO), 132–133

Hydroxyapatite ($\text{Ca}_{10}[\text{PO}_4]_6[\text{OH}]_2$), 284–286
 Hydroxyapatite nanowire (HAP-NW), 284–286
 Hydroxyl groups (OH groups), 110–111

I

Imaging XPS (IXPS), 514
 Immersion precipitation.
 See Nonsolvent-induced phase separation (NIPS)
 In situ modification, membrane modification by, 42–44
 In situ self-assembling coating method, 40–41
 Inductively coupled plasma–mass spectrometry (ICP-MS), 565
 Industrial Revolution, 177–178
 Infrared (IR), 506
 radiation, 553
 Infrared spectroscopy, 39
 and mapping, 515–516
 Initiated chemical vapor deposition (iCVD), 366
 Inkjet printing, 72
 inkjet printing–assisted surface grafting method, 88
 Inorganic all-solid-state electrolytes, 292–294
 Inorganic fouling, 44–47, 538–541.
 See also Organic fouling
 factors affecting scaling, 540–541
 mineral scaling on ZI-modified membranes, 46–47
 stages in scale formation, 539–540
 ZI polymers and ionic interactions, 45–46
 Inorganic materials, 2
 Inorganic modification, 136–145
 one-dimensional nanowires/nanotubes, 140–142
 two-dimensional nanosheets/nanoplates, 143–145
 zero-dimensional nanoparticles, 136–140
 Interfacial energy change, 616–617
 Interfacial polymerization method (IP method), 97–98, 476–479
 Intermediate chemical demineralization (ICD), 615
 Ion exchange capacity (IEC), 585
 Ion exchange membrane (IEM), 135, 158–159, 166–167, 575
 in electro dialysis and membrane capacitive deionization systems for water, 575–586
 for harvesting salinity gradient energy, 586–593
 capacitive mixing, 592–593
 reverse electro dialysis, 587–592
 Ion gel membranes, 8–9, 23–25
 containing AAILs and AHAs–based ionic liquids, 23–25
 ion gel membranes with epoxy amine gel networks, 25
 Ion-exchange, 613
 Ionic liquid (IL), 2–4
 ionic liquid–based membranes, 2
 CO_2 -reactive ionic liquid–based facilitated transport membranes, 17–23
 gas permeability of room-temperature ionic liquid–based membranes, 4–8
 ion gel membranes containing task-specific ionic liquids, 23–25
 ionic liquid–based CO_2 separation membranes, 8–17
 typical cations and anions constituting ionic liquids, 3f
 IRMOF-1, 223–224
 Iron-air batteries, 156
 Iron-chromium system (Fe–Cr system), 131–132
 Isothermal titration calorimetry (ITC), 523

J

Joule-Thomson effect (JT effect), 409

K

Knudsen diffusion, 197

L

Laminated object manufacturing (LOM), 76
 Lanthanum gallate (LSGM), 633
 Largest cavity diameter (LCD), 215–216
 Laser energy, 73

Laughing gas. *See* Nitrous oxide (N_2O)

Layered manufacturing, 73–74

Leveque's equation, 437–438

$\text{Li}_{1.3}\text{Al}_{0.3}\text{Ti}_{1.7}(\text{PO}_4)_3$ (LATP), 294

$\text{Li}_{6.75}\text{La}_3\text{Zr}_{1.75}\text{Ta}_{0.25}\text{O}_{12}$ (LLZTO), 292–294

LIBs. Lithium-ion batteries;
 See Lithium-ion batteries (LIBs)

Ligands, 219–220

Light microscopy, 543–544

Light sheet fluorescence microscopy (LSFM), 511

Lignin, 147–148

Liquid chromatography–mass spectrometry (LC–MS), 524

Liquid phase separation, 317

Lithium bis-
 (trifluoromethanesulfonyl) imide (LiTFSI), 289–290

Lithium carbonate, 632–633

Lithium-air batteries, 156

Lithium-ion batteries (LIBs), 269.
 See also Vanadium-air redox flow battery (VARFB)

separators

 ceramic-coated fibrous separators, 284–286

 increasing puncture strength of separators, 278–279

 increasing tensile strength of separators, 274–278

 mechanically strong separators, 273–279

 nonflammable separators, 280–288

 self-shutdown separators, 271–273

 separators with flame-retardant additives, 286–288

Loose NF (LNF), 374–375

Low calorific value gas (LCVG), 259–260

Low-molecular-weight (LMW), 435

Lumped parameter, 440

Lysine methacrylamide (lysAA), 364–365

Lysozyme, 48

M

m-phenylenediamine (MPD), 99, 100f, 376

- Magnesium-air batteries, 156
- Magnetic resonance imaging (MRI), 561–562
- Mapping technology, 467–468
- Mass spectrometry, 524, 565
- Material extrusion (ME), 74, 76–77
- Material jetting process (MJ process), 74–76
- Mathematical models for spiral-wound membrane, 405–408, 406t
- Matrimid, 182–185
- Melt spinning method, 185–187
- Membrane capacitive deionization (MCDI), 575, 583–586
 - applications, 583–584
 - membranes, 584–586
 - commercial membranes, 584–585
 - custom-made membranes, 585–586
 - systems, 575–586
- Membrane conductivity, 158–159
- Membrane distillation, 603
- Membrane electrode assembly (MEA), 158–159
- Membrane fabrication, 72, 533
 - via direct 3D printing, 81–82, 91t
- Membrane formation, modeling and simulation of, 468–479
 - dry casting, 476
 - interfacial polymerization, 476–479
 - phase separation, 469–476
- Membrane foulants, 357–358
- Membrane fouling, 499, 533. *See also* Surface fouling
 - characterization, 542–565, 543f
 - microscopic techniques, 544–553
 - spectroscopic and analytical techniques, 553–565
 - types of, 534–542
 - biofouling, 535–538
 - colloidal/particulate fouling, 541–542
 - inorganic fouling/scaling, 538–541
 - organic fouling, 541
- Membrane scaling, control strategies for, 613–618
 - antiscalants, 613–615
 - feedwater pretreatment, 613
 - operation mode of reverse osmosis system, 615–616
 - scaling-resistant reverse osmosis membrane, 616–618
- Membrane scaling and permeate flux, 612
- Membrane(s), 157, 306–308, 433
 - 3D printing in, 78–80, 79t
 - applications, 80–94
 - membrane fabrication via direct, 81–82, 91t
 - membrane surface modification via coating aided by, 83–94
 - classifications, 159–164
 - commercial Nafion membranes, 159–160
 - other membranes, 160–164
 - functional requirements of, 158–159
 - for gas phase separation, applications of, 311–316
 - gas separations, 215
 - membrane-based separation technology, 349, 433
 - membrane-scaling formation, theories for, 604–607
 - scaling kinetics, 605–607
 - scaling thermodynamics, 604–605
 - membrane-solute-solvent system, 435
 - modeling, 433
 - modification by in situ
 - modification, 42–44
 - module, 193–195
 - for organic solvent reverse osmosis, 321–322
 - performance-enhancing strategies for, 169–171
 - separation process, 1–2, 177–178, 305, 359
 - for solvent separation, applications of membranes, 317–322
 - technology, 329–330
- Mesh-adjustable molecular sieve (MAMS-1), 220–221
- Meso-erythritol (ME), 110–111
- Meso-scale methods, 467–468
 - coarse-grained methods, 467–468
 - DPD, 467
- Metagenomics, 525
- Metal ions, 305–306
- Metal-air battery, 156
- Metal-organic frameworks (MOFs), 215–216, 305–306, 330, 485–489
 - computational efforts on, 227–230
 - fabrication of, 216–220, 218f
 - channels for mass transfer, 217f
 - for gas separations, 220–227
 - membrane, 215–216
 - MOF-5 membrane, 216, 223–224
 - for pervaporation, 230–232
- 1-(methacryloyloxy) ethyl 1-carboxymethyl dimethyl ammonium (CBMA), 33–34
- 2-(methacryloyloxy) ethyl 3-sulfopropyl dimethyl ammonium (SBMA), 33–34
- [2-(methacryloyloxy) ethyl] trimethylammonium chloride (METMAC), 370
- Methacryloyloxyethyl phosphorylcholine (MPC), 33–34
- Methane (CH₄), 391, 408, 628–629
- Methoxycarbonyl (CH₃–O–CO), 535
- Methyl acetate (MA), 324
- Methyl benzoylformate (MBF), 287–288
- Methyl blue (MB), 374
- Methyl tert-butyl ether (MTBE), 321–322, 324
- Methylated silica hydrophobic colloid (Me-SiO₂), 319–320
- Methylene blue (MB), 340
- Metropolis Monte Carlo method, 467
- Micro-solid oxide fuel cell methane sensor, 639–646
 - current situation, 639
 - design and character of sensor, 640–642
 - sensor development, 640, 642–646
- Microbial biofouling, 55
- Microbial community, 525
- Microbial growth, 537
- Micro-channel formation, 243–244
- Microcystis aeruginosa*, 60–61
- Microfiltration (MF), 71–72, 317, 329–330, 501–502, 533
- Micro-monolithic ceramic fuel cells, 258–259

- Micro-monolithic membranes, 244
- Microorganisms, 535
- Micropores, 178–179
- Microscopic techniques, 511–513, 543–553
- AFM, 512, 549–550
 - CLSM, 513, 544–546
 - DICM, 552
 - epifluorescence microscopy, 550–552
 - ESEM, 552
 - SEM, 511–512, 546–549
 - TEM, 512, 552–553
 - visual inspection, 544
- Micro-structure characterization of carbon membrane, 198–200
- FIB and TEM, 200
 - Raman spectroscopy, 198
 - XPS, 198
 - XRD, 199–200
- Micro-structured ceramic membranes, 240–242
- Micro-tube, 240
- Mineral scaling, 604
- on ZI-modified membranes, 46–47
- Mixed ionic/electronic conductor (MIEC), 245, 630–631, 640–641
- Mixed matrix membranes (MMM), 330–331, 435–436
- modeling of, 454–459
- Mixing entropy battery (MEB), 592.
- See also* Redox flow battery (RFB)
- Module construction, 193–195
- components for hollow fiber membrane module, 194f
- Molar balance, 400
- Molecular dynamics simulation (MD simulation), 466
- Molecular force field, 466
- Molecular modeling and simulation, 463–468
- on hollow-fiber membrane, 479–482
 - in membrane design, 482–489
 - graphene and two-dimensional carbon material, 482–485
 - metal-organic membranes, 485–489
 - ZIF, 485–489 - of membrane formation, 468–479
 - types of simulation methods, 464–468
 - atomistic-scale methods, 466–467
 - electronic scale methods, 464–466
 - meso-scale methods, 467–468
 - meso-scale molecular simulations, 468 - Schrodinger equation, 468
- Molecular sieving, 195–197
- Molecular weight cutoff (MWCO), 319–320, 329–330
- Molten carbonate fuel cells (MCFCs), 627–628
- Molybdenum disulfide (MoS₂), 143
- Monomeric silica, 612
- Monovalent selectivity, 582
- Monovalent-selective electro dialysis membranes, 580
- Monte Carlo simulation, 467
- Multichannel design (micro-monolithic design), 248–251
- Multiple effect distillation, 603
- Multistage flash distillation, 603
- Multivariate analyses, 521
- ## N
- N,N,N-2,2,6,6-heptamethylpiperidinyloxy-4-ammonium chloride/viologen derivative N, N'-dimethyl-4,4-bipyridinium dichloride (TEMPTMA/MV), 132–133
- N,N-diethylethylenediamine, 368
- N,N-bis(acryloyl) cystamine (BAC), 365–366
- N-(3-dimethylaminopropyl) methacrylamide (DMAPMAPS), 365–366
- N-(3,4-dihydroxyphenethyl) methacrylamide, 365–366
- N-aminoethyl piperazine (AEP), 110
- N-aminoethyl piperazine propane sulfonate (AEPSPS), 110, 368–369, 376
- Nafion, 627–628
- commercial Nafion membranes, 159–160
 - membrane, 135–136
 - Nafion 117 membrane, 160–162, 164–165, 168
 - nafion/sulfonated-organosilica composite membranes, 139
- Nanofibers, 71–72
- Nanofiltration (NF), 97, 317, 329–330, 357–358, 433–434, 533, 613
- pore flow modeling for, 443–448
- Nanomaterials, 330
- Nanyang Technological University (NTU), 71–72
- National Security Agency (NSA), 628
- Natural gas, 628
- sweetening, 205–207
- Natural organic matter (NOM), 368
- treatment in water, 368–370
- Natural rubber (NR), 636
- New micro-monolithic solid oxide fuel cell, 258–263
- greenhouse gas abatement using ceramic fuel cells, 260
 - three-dimensional characterization of ceramic membrane, 260–263
- Newton's equation of motion, 468
- Next-generation oxygen separation, 251–252
- Next-generation purification technology, 215
- Nickel (Ni), 305–306, 630
- Nitrogen (N₂), 408
- Nitrous oxide (N₂O), 260
- Non-pressure-driven processes, 329–330
- Nonaqueous flow battery, 133–134
- Noncovalent modification, 146–148
- Nonflammable separators, 280–288
- Nonfluorinated membranes, 135–136
- Nonlinear algebraic equation, 396–398
- Nonsolvent-induced phase inversion (NIPS), 42, 469, 472–476
- Nonwoven fabrics, 269
- Novel spacer geometries, 415, 424–425
- Nuclear magnetic resonance spectroscopy (NMR spectroscopy), 517–518, 561–562
- ## O
- O-ring, 635–636
- Offline characterization of surface fouling, 511–521
- CA, 519–520

- data mining via statistical analysis, 521
 - microscopic methods, 511–513
 - spectroscopic methods, 513–519
 - TOF-SIMS, 520
 - Ogston model, 15–16
 - Oily wastewater treatment, 370–373
 - Oligomers, 609–610
 - One-dimension(1D)
 - film theory, 436–438
 - mathematical model, 396
 - models, 395–399, 415–418
 - concentration profile in boundary layer, 416f
 - typical reverse osmosis membrane desalination process, 418f
 - nanowires/nanotubes, 136, 140–142
 - Online characterization of surface fouling, 504–511
 - ATR technology, 506
 - DO, 504–505
 - EIS, 509–510
 - fluorescence spectroscopy, 507–509
 - FTIR spectroscopy, 506
 - LSFM, 511
 - OCT, 505
 - QCM-D, 510
 - Raman spectroscopy, 506–507
 - SPR, 510–511
 - Open-channel micro-structure design, 247–248
 - Optical coherence tomography (OCT), 424–425, 505
 - Ordinary differential equation model (ODE model), 417
 - Organic carbon detector (OCD), 524
 - Organic fouling, 47–53, 499, 541, 542t. *See also* Inorganic fouling
 - environmental conditions and organic foulants, 51–53
 - mechanisms of zwitterionic polymers' resistance to organic fouling, 48–51
 - Organic modification, 145–148
 - covalent modification, 145–146
 - noncovalent modification, 146–148
 - Organic nitrogen detector (OND), 524
 - Organic porous materials, 331–333
 - Organic solvent mixtures,
 - pervaporation of, 324
 - Organic solvent nanofiltration (OSN), 306
 - membranes, 319–320
 - Organic solvent reverse osmosis (OSRO), 306
 - membranes for, 321–322
 - Organosilica membranes, 306–308
 - crystalline structure and amorphous structure, 307f
 - permeation properties, 308f
 - pervaporation dehydration using, 323
 - preparation of, 308f
 - silicon-based membranes with amorphous structure, 307t
 - ORR. Oxygen reduction reaction;. *See* Oxygen reduction reaction (ORR)
 - Osmotic pressure-based models, 436–448
 - detailed two-dimensional model, 443–448
 - flow through rectangular channel, 439–443
 - one-dimensional film theory, 436–438
 - two-dimensional mass transfer boundary layer model, 438–439
 - Osmotic pressure—controlling phenomenon, 435
 - Overall mass transfer coefficient, 399
 - Oxidative coupling of methane (OCM), 253
 - Oxidized multiwalled carbon nanotubes (O-MWCNTs), 590–591
 - 2,2'-oxybis-ethylamine (2,2'-OEL), 105, 105f
 - Oxyfuel combustion method, 205, 245
 - Oxygen (O₂), 239, 309–311, 629–630
 - permeation, 164–166
 - Oxygen evolution reaction (OER), 156–157
 - Oxygen permeable membranes (OPMs), 245
 - catalytic reactor based on, 253–254
 - and membrane reactor, 245–254
 - catalytic reactor based on oxygen-permeable membrane, 253–254
 - design of high-performance oxygen permeation membrane, 247–252
 - oxygen transport in high-temperature ion conductors, 245–247
 - Oxygen reduction reaction (ORR), 156–157
- P**
- Palladium (Pd), 640
 - Palm oil mill effluents (POME), 628–629, 639
 - Particle image velocimetry, 424–425
 - PEG diglycidyl ether (PEG-DGE), 362
 - Perfluorinated sulfonic acid, 146
 - Performance-enhancing strategies for membranes, 169–171
 - Permeate flux, 416, 433, 436, 441
 - membrane scaling and, 612
 - Permeate spacer, 413–414
 - Permeate volumetric flow rate, 417
 - Permeation, 433–434
 - Permselectivity of CO₂ through RTIL-based membranes, 6–7
 - Perovskite ceramics, 633
 - Pervaporation (PV), 306
 - application to, 322–324
 - dehydration using organosilica membranes, 323
 - organic solvent mixtures, 324
 - dehydration using organosilica membranes, 323
 - metal-organic framework membranes for, 230–232, 230f
 - Petroleum resources, 177–178
 - pH titration method, 523
 - Phase inversion method, 97–99, 240, 243
 - Phase inversion—assisted extrusion technique, 250–251
 - Phase inversion—assisted fabrication technique, 242–243
 - Phase separation, 469–476
 - NIPS, 472–476
 - PIPS, 476
 - TIPS, 469–472

- Phenol-formaldehyde-resin (PFR), 288
 Phenolic alcohols (OH), 535
 Phosphate anionic groups (PC), 351–352
 Phosphonate, 33–34
 Phosphonic acid, 578
 Phosphorylcholine-based polymers (PC), 33–34
 Phosphotungstic acid (PWA), 147
 Photo-induced polymerization, 37–39
 Photoacoustic spectroscopy (PAS), 562
 Photopolymerization, 77
 Photovoltaic method (PV method), 578
 Physical mass transfer model, 479–480
 Piperazine (PIP), 99
 Planar disk type, 247–248
 Planck's constant, 557
 Plasma-enhanced chemical vapor deposition (PECVD), 306, 309–311
 Plasma-grafting polymerization, 364–365
 Plasma-induced polymerization, 37–39
 Platinum (Pt), 640
 PMP-diluent system, 481, 481*f*
 Poiseuille flow, 197
 Poly(sulfobetaine methacrylate) (PSBMA), 339
 Poly-N,N'-dimethylaminoethyl methacrylate (PDMAEMA), 49
 Poly(2-hydroxyethyl methacrylate) (pHEMA), 50–51
 Poly(2-methacryloyloxyethyl phosphorylcholine) (PMPC), 351
 Poly(2,6-dimethyl-1,4-phenylene oxide) (PPO), 589–590
 Poly(4-methyl-1-pentene) (PMP), 481
 Poly(acrylic acid) (PAA), 593
 Poly(acrylonitrile) (PAN), 294
 Poly(amic acid) (PAA), 284–286
 Poly(carboxybetaine methacrylate) (PCBMA), 351
 Poly(diallyldimethyl ammonium chloride) (PDDA), 589–590, 593
 Poly(ethersulfone) (PES), 90–94, 360, 469–470
 Poly(ethylene glycol) (PEG), 33, 280–281, 349–350
 Poly(ethylene glycol) dimethacrylate (PEGDMA), 287–288
 Poly(lactide-co-glycolide) (PLGA), 479–480
 Poly(phenylene oxide) (PPO), 182–185
 Poly(sodium 4-styrene sulfonate) (PSS), 593
 Poly(stearyl methacrylate)-block-poly 2-(dimethylamino) ethyl methacrylate (PSM-*b*-PDM), 375
 Poly(styrene-co-ethylene glycol methacrylate-co-SBMA), 42
 Poly(sulfobetaine methacrylate) (PSBMA), 39–40, 351
 Poly(vinyl alcohol) (PVA), 275–277, 360
 Poly(vinylidene fluoride-co-chlorotrifluoroethylene) (PVDF-CTFE), 288
 Poly(vinylidene fluoride) (PVDF), 360, 506
 Polyacrylates, 613–614
 Polyacrylonitrile (PAN), 360
 Polyacyl chloride monomers, 122–123
 Polyamide (PA), 97, 358
 Polyampholytes, 34–36, 34*f*, 351, 355–356
 architecture of polyampholyte structures, 355*f*
 polyampholyte sequences, 356*t*
 Polyaniline (PANI), 162–163
 Polybenzimidazole (PBI), 271–273
 nonflammability of, 271–273
 Polybetaines, 34*f*, 56, 351–355
 polybetaine zwitterion structures, 353*t*
 Polycarbosilane (PCS), 309
 Polyepichlorohydrin (PECH), 589–590
 Polyestersulfone (PES), 39, 110–111, 279, 330
 Polyethylene (PE), 269–270, 578
 Polyethylene oxide (PEO), 289–290
 Polyethylenimine (PEI), 160–162, 374
 Polyformaldehyde–cellulose nanofiber (POM-CNF), 277–278
 Polyimides, 182–185
 Polymeric membranes, 333–334
 fabrication, 182–185
 Polymeric preparation membrane, 185–188
 methods of, 186*f*
 Polymerization-induced phase separation (PIPS), 469, 476
 Polymerized ionic liquid membranes (poly(IL) membranes), 8–9, 11–13
 Polymers with intrinsic microporosity (PIMs), 8–9
 Polyolefin separators, 271–273
 Polyphosphonates, 613–614
 Polyphosphoric acid (PPA), 288
 Polypropylene (PP), 39–40, 269–270
 Polystyrene, 578
 Polysulfone (PS), 101–105
 Polysulfone (PSU), 82, 330, 349–350, 578
 Polytetrafluoroethylene, 146
 Polyurethane (PU), 72
 Polyvinyl alcohol (PVA), 88, 435, 586
 Polyvinylchloride (PVC), 589
 Polyvinylidene difluoride (PVDF), 39–40, 220–221, 330, 470
 Pore flow modeling for nanofiltration, 443–448
 Pore flow transport, 452–454
 Pore limiting diameter (PLD), 215–216
 Pore size distribution (PSD), 228–229
 Pore tailoring technique, 191–193
 Pore-filling membranes, 586
 Porous hybrid materials, 331–333
 Porous materials, 331–333
 Porous polymer separators, 269
 Postcombustion capture, 203–205
 Postoxidation treatment, 191
 Powder bed fusion (PBF), 74, 77
 Precursor selection for carbon membrane, 182–185
 chemical structures of commonly used polymeric precursors, 184*t*
 Pressure swing adsorption (PSA), 245

- Pressure-driven processes, 329–330
 Pressure-resistant ionic liquid-based membranes (poly(RTIL) membranes), 11–17
 ionic liquid-based gel membranes, 13–16
 polymerized ionic liquid membranes, 11–13
 thin ion gel membrane, 16–17
 Pressure-retarded osmosis (PRO), 371–372
 Primary RO modules, 582–583
 Profiled electro dialysis membranes, 579–580
 Prokaryotic cells, ZI polymers and interaction with, 56–59
 1,3-propanesultone (1,3-PS), 110
Proteobacteria, 535
 Proton exchange membrane fuel cells (PEMFCs), 627–628
Pseudomonas, 537–538
Pseudomonas aeruginosa, 58–59
 Purification technology, 177–178
 2,4,6-pyridinetri-carboxylic acid chloride (PTC), 119–121
 Pyrolysis, 178–179, 188–190
- Q**
 Quartz crystal microbalance with dissipation (QCM-D), 510
- R**
 Ram extrusion process, 240
 Raman spectroscopy, 198, 506–507, 517, 557–560, 559*t*, 560*f*
 Rapid heat treatment (RHT), 222
 Rapid prototyping, 73–74
 Rayleigh-Taylor instability theory, 244
 Rectangular channel, flow through, 439–443
 Redox flow battery (RFB), 131, 155
 aqueous flow battery systems with typical redox couples, 133*t*
 development of, 131–135
 structure and working principle of, 132*f*
 Refinery processes, 201–203
 Regression analyses, 521
 Renewable energy sources, 131, 155
 Resistance-in-series model, 503–504
 Reverse electro dialysis (RED), 575, 587–592
- Reverse osmosis (RO), 37–39, 97, 317, 329–330, 357–358, 413, 433–434, 501–502, 533, 576
 membrane, 603
 control strategies for membrane scaling, 613–618
 established theories for membrane-scaling formation, 604–607
 future challenges for mineral-scaling control, 618–620
 membrane scaling in brackish groundwater desalination, 607–612
 membrane modules
 1D models, 416–418
 2D models, 418–422
 3D models, 422–429
 research direction, 415*f*
 spiral-wound membrane for reverse osmosis, 414*f*
 operation mode of RO system, 615–616
 Reversed-phase chromatography, 524
 Reversible addition-fragmentation chain transfer (RAFT), 352
 Rhodium (Rh), 640
 16S RNA sequence, 525
 Robeson upper bound, 2
 Rocket propellants, 245
 Room-temperature ILs (RTILs), 2.
 See also Amino acid ILs (AAILs)
 gas permeability of room-temperature ionic liquid-based membranes, 4–8
 permselectivity of CO₂ through RTIL-based membranes, 6–7
 solubility selectivity of CO₂ in, 6–7
 Root means square (RMS), 550
- S**
 Saline feed stream, 576
Salmonella enterica, 86–88
 Salty water desalination, 603
 Samarium oxide (Sm₂O₃), 632
 Samarium-doped ceria (SDC), 632
 Sankey diagram, 165–166, 166*f*
 Scale formation, stages in, 539–540
 Scaling control strategies, 604
- Scaling kinetics, 605–607
 Scaling mechanisms, 424
 Scaling thermodynamics, 604–605, 605*f*
 Scaling-resistant reverse osmosis membrane, 616–618
 Scandia-stabilized zirconia (ScSZ), 632
 Scandium oxide (Sc₂O₃), 632
 Scanning electron microscopy (SEM), 41–42, 260–262, 271–273, 511–512, 546–549, 548*f*, 606
 Seawater, 603
 Seawater reverse osmosis (SWRO), 417
 Secondary RO modules (SRO modules), 615
 Securing adequate water resources, 329
 Selective laser melting, 77
 Selective laser sintering, 73, 77
 Selemion CSO, 590
 Self-assembly technique, 147
 Self-shutdown separators, 271–273
 Self-supporting carbon membrane, 180–182
 Semisolid flow cell, 134
 Sensor development, 642–646
 calibration of methane concentration, 644–645
 composites of solid oxide fuel cell, 643*t*
 measurement of methane concentration in biogas using gas chromatography, 645
 sensor performance, 645–646
 Separation energy of solvent mixture, 317–319
 Separators
 comparison of mechanical strength of common polymer separator, 275*t*
 increasing puncture strength of, 278–279
 increasing tensile strength of, 274–278
 Sericin (SC), 110
 Sheet lamination (SL), 74, 76
 Sherwood number (*Sh*), 417, 434, 442
Shigella flexneri, 86–88
Shigella sonnei, 86–88

- Silica (SiO₂), 2, 88, 136–137, 306–308
- Silica nanoparticles (siNPs), 48
- Silica-oxygen-borate (Si-O-B), 279
- Silica-oxygen-silica (Si-O-Si), 279
- Silicon carbide (SiC), 306, 314, 638–639
- silicon carbide-based membranes, 309
- Silicon-based subnanoporous membranes, 306
- application to pervaporation, 322–324
 - applications of membrane for gas phase separation, 311–316
 - applications of membranes for solvent separation, 317–322
 - development of, 306–311
 - organosilica membranes, 306–308
 - PECVD, 309–311
 - silicon carbide-based membranes, 309
- Silicone, 306–308
- silicon oxide-based membranes for gas separation, 311–314
 - silicon-based materials, 306–308
 - silicon-based nonoxide membranes for gas separation, 314
- Siloxanes, 350–351
- Silver nanoparticles (AgNP), 48, 90
- Size-exclusion chromatography, 524
- Sodium (Na), 547–549
- Sodium alginate (SA), 106, 612, 619–620
- Sodium carbonate, 632–633
- Sodium chloride (NaCl), 97–98, 446
- Sol-gel coating method, 219
- Solar energy, 177–178
- Solid electrolyte interface (SEI), 269–270
- Solid free-form fabrication, 73–74
- Solid oxide fuel cells (SOFCs), 239, 255–256, 627–629, 634, 636
- Solid polymer electrolytes (SPEs), 289–291
- Solid-phase fluorescence EEM (SPF-EEM), 507–509
- Solid-phase fluorescence spectroscopy (SPF), 514–515
- Solid-phase UV–vis spectroscopy, 514
- Solubility selectivity of CO₂ in RTIL, 6–7
- Solute diffusivity, 418–419
- Solution spinning, 185–187
- Solution-diffusion model, 434–435
- Solvent separation, membranes
 - applications for, 317–322
 - evaluation of separation energy of solvent mixture, 317–319
 - membranes for organic solvent reverse osmosis, 321–322
 - organic solvent nanofiltration membranes, 319–320
- Solvent-based slurry
 - stereolithography, 85–86
- Specific density, 398
- Spectroscopic methods, 513–519
 - analytical techniques, 553–565
 - FTIR, 553–554
 - Raman spectroscopy, 557–560
 - XPS, 557
 - XRD technique, 554–556
 - XRF technique, 556
 - EDS, 513
 - infrared spectroscopy and mapping, 515–516
 - NMR, 517–518
 - other techniques, 560–565
 - bioluminescence, 561
 - fluorometry techniques, 560–561
 - gravimetric analysis, 562–564
 - mass spectrometric and chromatographic techniques, 565
 - NMR spectroscopy, 561–562
 - PAS, 562
 - properties, 523
 - chromatography, 524
 - Raman imaging, 517
 - solid-phase UV–vis spectroscopy, 514
 - SPF, 514–515
 - THz-TDS, 516–517
 - XAS, 519
 - XPS, 513–514
 - XRD, 518–519
- Sphingomonads*, 538
- Spinning process, 242–243
- Spiral-winding process, 273–274
- Spiral-wound membrane (SWM), 393, 413–414
- challenges and future direction in modeling of, 408–409
- effect of heat transfer within module, 409
 - multicomponent separation, 408
 - effect of pressure drop in feed and permeate channel, 408–409
 - construction and flow configuration of, 394
 - gas separation membrane, 392*t*
 - hollow-fiber and spiral-wound membrane, 393*t*
 - modeling strategies, 394–408
 - 1D models, 396–399
 - 2D models, 399–402
 - 3D models, 402–405
 - crossflow permeation membrane leaf, 395*f*
 - mathematical models for, 405–408
 - spiral-wound membrane module, 395*f*
- Stacked plate process, 273–274
- Staphylococcus aureus*, 368–369
- Statistical analysis, data mining via, 521
- Steam methane reforming method (SMR method), 177–178
- Steric hindrance effect, 359
- Strong Coulomb force, 3–4
- Structure patterning, 83
- Succinonitrile (SN), 290
- Sulfated polyvinyl alcohol (sPVA), 589–590
- Sulfates (SO₄), 538–539
- Sulfobetaine (SB), 351–352
- Sulfobetaine methacrylate (SBMA), 39–40, 360–361
- Sulfobetaine-based polymers (SB), 33–34
- Sulfonated poly(ether ether ketone) (SPEEK), 135–136, 162–163, 589–590
- Sulfonated poly(ether sulfone) (SPES), 135–136
- Sulfonated poly(phthalazinone ether ketone) (SPPEK), 135–136
- Sulfonated polyethersulfone (sPES), 591
- Sulfonated polyimide (SPI), 135–136

- Sulfonic acid, 578
- Sum frequency generation
vibrational spectroscopy (SFG
vibrational spectroscopy), 52
- Supported carbon membrane,
180–181, 187–188
- Supported ionic liquid membranes
(SILMs), 8–11
containing aprotic heterocyclic
anion-based ionic liquids,
21–22
containing ionic liquids with
carboxylate anions, 22–23
- Surface crystallization, 608
- Surface foulants
characterization of extracts from,
521–525
biological properties, 525
chemical composition, 522
extraction of surface foulants, 522
physicochemical properties,
522–523
spectroscopic properties, 523
compression of, 502–503
extraction, 522
maturation and retardation of, 503
- Surface fouling. *See also* Membrane
fouling
modeling of, 500–504
CP boundary layer, 503–504
filtration laws, 500–502
offline characterization of,
511–521
CA, 519–520
data mining via statistical
analysis, 521
microscopic methods, 511–513
spectroscopic methods, 513–519
TOF-SIMS, 520
online characterization of,
504–511
ATR technology, 506
DO, 504–505
EIS, 509–510
fluorescence spectroscopy,
507–509
FTIR spectroscopy, 506
LSFM, 511
OCT, 505
QCM-D, 510
Raman spectroscopy, 506–507
SPR, 510–511
- Surface plasmon resonance (SPR),
510–511
- Surface quaternization, modification
by, 367–368
- Surface-enhance Raman spectroscopy
(SERS), 507, 557–558
- Surface-initiated polymerization (SI
polymerization), 37–39
- Surface-patterned alumina ceramic
membrane, 86
- Sustainable energy, 177–178
- Sustainable power generation, 155
- Syngas, 628
- ## T
- Tape casting, 247–248
- Task-specific ILs (TSILs), 17
- Terahertz time-domain spectroscopy
(THz-TDS), 516–517
- Tetra-armed polyethylene glycol
(tetra-PEG), 14–15
- Tetraethoxysilane (TEOS), 308
- Tetrahydrofuran (THF), 231–232
- 2,2,6,6-tetramethylpiperidinyloxyl
(TEMPO), 132–133
- Textile wastewater treatment,
374–375
- Thermal expansion coefficients
(TECs), 631
- Thermally induced phase separation
(TIPS), 277–278, 469–472
- Thin ion gel membrane, 16–17
- Thin-film composite (TFC), 37–39,
72–73, 97
commercial thin-film composite
membranes, 100–101
comparison of novel TFC
membranes with commercial
membranes, 101–108, 124*t*
nanofiltration or reverse osmosis
membrane, 99*f*
novel acyl chloride monomers,
115–123
novel amine monomers, 101–115
- Three-dimensional models (3D
models), 395–396, 402–405,
415, 422–429, 544
2D CFD modeling, 423*t*
3D CFD simulation in spiral-
wound membranes, 427*t*
biofilm distribution, 427*f*
CO₂ gas concentration, 405*f*
meshing of spiral-wound
membrane, 404*f*
movement of solute in feed
channel, 428*f*
perforated spacer, 426*f*
- Three-dimensional printing
technology (3D printing
technology), 71, 580
advantages and limitations, 78,
78*t*
applications in membrane
technology, 80–94
classification, 73–80, 74*t*
binder jetting, 76
DED, 74
material extrusion, 76–77
MJ, 74–76
powder bed fusion, 77
sheet lamination, 76
vat photopolymerization, 77
role and trend in membrane
technology for water
applications, 78–80, 79*t*
working principle, 75*f*
- Three-dimensional spatial
distribution (3D spatial
distribution), 260–262
- Titania (TiO₂), 136–137
- Titanium alloys, 62–63
- Titanium dioxide (TiO₂), 582
- Total dissolved solids (TDS),
452–453, 607–608
- Transient one-dimensional gel layer
controlling model, 449–452
coupled with film theory,
449–452
coupled with pore flow transport,
452–454
- Transmission electron microscopy
(TEM), 198, 200, 260–262,
288, 512, 552–553
- Transport mechanisms, 168–169
- Transport phenomena-based models,
433–434, 436–448
osmotic pressure-based models,
436–448
- Triaminopyrimidine (TAP), 106
- 3-(triethoxysilyl) propan-1-amine
(PA-Si), 313–314
- 3-(triethoxysilyl)-N,N-
dimethylpropane-1-amine
(TA-Si), 313–314
- 3-(triethoxysilyl)-N-methylpropan-1-
amine (SA-Si), 313–314
- Trimellitic anhydride chloride (TAC),
118
- Trimers, 609–610
- Trimesoyl chloride (TMC), 99, 376

Trimethyl borate (TMB), 279
 Trimethylsilyl (TMS), 182–185
 Triphenyl phosphate (TPP),
 286–287
 Triple-phase boundaries (TPB),
 634–635
 Triptycene-2,3,6,7,14,15-hexaacyl
 chloride (THC), 123
 Tris(2-aminoethyl) amine (TAEA),
 106
 Tubesheet functions, 193–195
 Tungsten trioxide (WO₃), 136–137
 Tuning pore dimension, methods
 for, 190–193
 Turbostratic carbon structure,
 178–179
 Turbulent flow, 437
 Two-dimension (2D), 395–396,
 399–402, 415, 418–422
 biofilm development, 420*f*
 carbon material, 482–485
 desalination cell, 423*f*
 fluid domain indicating boundary
 locations and channel regions,
 422*f*
 imaging techniques, 260–262, 550
 mass transfer boundary layer
 model, 438–439
 mathematical model, 402
 nanosheets/nanoplates, 136,
 143–145
 spiral-wound membrane feed
 channel, 421*f*
 Two-dimensional correlation
 spectroscopy (2DCOS), 521
 Two-dimensional model, 443–448

U

U.N. Department of Economic and
 Social Affairs, 177–178
 Ultrafiltration (UF), 39, 85–86,
 98–99, 317, 329–330,
 424–425, 433–434,
 501–502, 533
 antifouling and antibacterial
 properties, 334–339
 antifouling studies, 336*t*
 cross-sectional SEM images, 337*f*
 SEM images, 337*f*
 dye rejection, 339–341
 mixed matrix membranes
 micro-enhancers and
 nanoenhancers, 331–334
 other applications, 341–344, 343*t*

Ultramicropores, 178–179, 190
 Ultrasonic additive manufacturing
 (UAM), 76
 Ultraviolet (UV), 74–76, 364–365,
 507–509
 Underwater oil contact angle (OCA),
 88
 Unsteady shear strategies, 415, 429
 UV–vis spectroscopy, 514

V

Vanadium ion crossover, 166–168,
 167*f*
 Vanadium redox flow battery
 (VRFB), 135, 155–156
 essential role of membrane in,
 135–136
 inorganic modification, 136–145
 organic modification, 145–148
 Vanadium-air redox flow battery
 (VARFB), 156–159. *See also*
 Lithium-ion batteries (LIBs)
 functional requirements of
 membranes, 158–159
 mechanisms and influences of
 species crossover, 164–169
 oxygen permeation, 164–166
 vanadium ion crossover,
 166–168
 water transport, 168–169
 membrane classifications,
 159–164
 performance-enhancing strategies
 for membranes, 169–171
 working principles, 158, 158*f*
 Vapor-induced phase separation
 (VIPS), 42–43
 Vat photopolymerization, 74, 77
Vibrio harveyi, 561
 Vinyl sulfonic acid (VSA), 370
 Viscous flow. *See* Poiseuille flow

W

Wastewater treatment, 329

Water

demineralization
 ion exchange membranes in
 electrodialysis, 575–586
 membrane capacitive
 deionization systems,
 575–586
 molecule, 139
 quality, 575
 reclamation, 349, 368

shortage, 375
 transport, 168–169
 treatment, 71
 Water contact angle (WCA), 88
 Water quality effects on mineral
 scaling, 610–612
 Wind energy, 177–178
 World Energy Council, 177–178

X

X-ray absorption near edge structure
 (XANES), 519
 X-ray absorption spectroscopy (XAS),
 519
 X-ray computed tomography (X-CT),
 260–262
 X-ray diffraction (XRD), 198–200,
 518–519, 554–556, 555*f*
 X-ray fluorescence technique (XRF
 technique), 556
 X-ray photoelectron spectroscopy
 (XPS), 39, 198, 513–514,
 557, 558*f*, 559*t*
 X-ray technique, 547, 556

Y

Yttria-stabilized zirconia (YSZ),
 630–632
 Yttrium-doped barium zirconate, 256

Z

Zeolite imidazolate framework (ZIF),
 482, 485–489
 Zeolites, 2, 305–306
 Zero-dimensional nanoparticles (0D
 nanoparticles), 136–140
 Zeta potential, 523
 Zinc chloride (ZnCl₂), 447
 Zirconia oxide (ZrO₂), 632
 Zirconium oxide (ZrO₂), 635
 ZLNF. *See* Zwitterion-modified NF
 ZrO₂ nanotubes (ZrNT), 141–142
 Zwitterion-modified membranes
 antifouling mechanisms, 357–359
 classification of membrane
 foulants, 357–358
 establishment of hydration layer
 on membrane surface,
 358–359
 steric hindrance effect, 359
 applications of, 368–376
 desalination, 375–376
 oily wastewater treatment,
 370–373

- textile wastewater treatment, 374–375
- treatment of natural organic matter in water, 368–370
- classification of zwitterionic polymers, 351–356
- preparation of zwitterion-modified membranes, 360–368
- modification by blending of zwitterionic polymers, 360–363
- modification by grafting, 363–366
- modification by surface coating, 366
- modification by surface quaternization, 367–368
- Zwitterion-modified NF (ZLNF), 374–375
- Zwitterionic acrylate monomer coating, 72
- material, 90
- Zwitterionic polymers (ZI polymers), 33, 350–351
 - betaine-like monomers, 35*t*
 - classification of, 351–356
 - polyampholytes, 355–356
 - polybetaines, 351–355
 - and inorganic fouling, 44–47
- modification by blending of, 360–363
- and organic fouling, 47–53
- organic fouling, biofouling, and mineral scaling on polymer surfaces, 36*f*
- ZI membrane fabrication and characterization, 37–44
- grafting processes for membrane modification, 37–42
- membrane modification by in situ modification, 42–44
- zwitterionic polymers and biofouling, 53–63
- Zwitterionic triamine (ZTM), 108